Radiol Phys Technol (2011) 4:173–179
DOI 10.1007/s12194-011-0118-1

Estimation of focal and extra-focal radiation profiles based on Gaussian modeling in medical linear accelerators

Shigeo Anai · Hidetaka Arimura · Katsumasa Nakamura · Fujio Araki · Takaomi Matsuki · Hideki Yoshikawa · Satoshi Yoshidome · Yoshiyuki Shioyama · Hiroshi Honda · Nobuo Ikeda

Received: 31 October 2010 / Revised: 6 March 2011 / Accepted: 8 March 2011 / Published online: 24 March 2011

Abstract The X-ray source or focal radiation is one of the factors that can degrade the conformal field edge in stereotactic body radiotherapy. For that reason, it is very important to estimate the total focal radiation profiles of linear accelerators, which consists of X-ray focal-spot radiation and extra-focal radiation profiles. Our purpose in this study was to propose an experimental method for estimating the focal-spot and extra-focal radiation profiles of linear accelerators based on triple Gaussian functions. We measured the total X-ray focal radiation profiles of the accelerators by moving a slit in conjunction with a photon field *p*-type silicon diode. The slit width was changed so that the extra-focal radiation could be optimally included in the total focal radiation. The total focal radiation profiles of an accelerator at 4-MV and 10-MV energies were approximated with a combination of triple Gaussian functions, which correspond to the focal-spot radiation, extra-focal radiation, and radiation transmitted through the slit assembly. As a result, the ratios of the Gaussian peak value of the extra-focal radiation to that of the focal spot for 4 and 10 MV were 0.077 and 0.159, respectively. The peak widths of the focal-spot and extra-focal radiation profiles were 0.57 and 25.0 mm for 4 MV, respectively, and 0.60 and 22.0 mm for 10 MV, respectively. We concluded that the proposed focal radiation profile model based on the triple Gaussian functions may be feasible for estimating the X-ray focal-spot and extra-focal radiation profiles.

Keywords Medical linear accelerator · X-ray focal spot · Extra-focal radiation · SBRT (stereotactic body radiation therapy) · Gaussian modeling

S. Anai · K. Nakamura · H. Yoshikawa · S. Yoshidome
Department of Radiology, Kyushu University Hospital at Beppu, Tsurumihara Tsurumi, Beppu, Oita 874-0838, Japan

S. Anai · N. Ikeda
Department of Applied Quantum Physics and Nuclear Engineering, Graduate school of Engineering, 744 Motooka Nishi-ku, Fukuoka 819-0395, Japan

H. Arimura
Department of Health Sciences, Faculty of Medical Sciences, Kyushu University, 3-1-1 Maidashi, Higashi-ku, Fukuoka 812-8582, Japan

F. Araki
Department of Health Sciences, School of Medicine, Kumamoto University, 4-24-1 Kuonji, Kumamoto 862-0976, Japan

T. Matsuki
Department of Medical Technology, Kyushu University Hospital, 3-1-1 Maidashi, Higashi-ku, Fukuoka 812-8582, Japan

Y. Shioyama
Department of Heavy Particle Therapy and Radiation Oncology, Graduate School of Medical Sciences, Kyushu University, 3-1-1 Maidashi, Higashi-ku, Fukuoka 812-8582, Japan

H. Honda
Department of Clinical Radiology, Graduate School of Medical Sciences, Kyushu University, 3-1-1 Maidashi, Higashi-ku, Fukuoka 812-8582, Japan

H. Arimura (✉)
Division of Medical Quantum Science, Department of Health Sciences, Faculty of Medical Sciences, Kyushu University, 3-1-1 Maidashi, Higashi-ku, Fukuoka 812-8582, Japan
e-mail: arimura@shs.kyushu-u.ac.jp

1 Introduction

Stereotactic body radiation therapy (SBRT) is a precise irradiation method for an extracranial lesion by use of a small number of high-dose fractions [1]. The advantages of SBRT for treating lung tumors are a shortened treatment course that requires fewer trips to the clinic than does a conventional treatment, and the improvement of tumor coverage and normal tissue sparing allowed by greater precision of the setup [2]. Therefore, steep dose gradients outside a target volume must be required with higher precision, because a high dose per fraction should be delivered to a small tumor within a conformal irradiation field in SBRT.

The X-ray source or focal spot is one of the factors which can degrade the conformal field edge in the SBRT. Wang and Leszczynski [3] reported that the dose profile penumbra depends on the X-ray focal-spot size and shape. Therefore, if the focal-spot size became wider, the dose profile penumbra would be larger. As a result, the conformal edge would be blurred. On the other hand, radiation treatment planning (RTP) algorithms based on Monte Carlo simulation have been widely used in several commercial RTP systems [4–8]. In Monte Carlo simulations, the X-ray focal-spot size and shape of each linear accelerator are required for estimation of a more accurate three-dimensional dose distribution in lung cancer patients for SBRT. For that reason, it is very important to estimate the focal-spot radiation of linear accelerators.

Some researchers hypothesized that the total focal radiation consisted of focal-spot radiation and extra-focal radiation [9–11]. Because the characteristics of the focal-spot and extra-focal radiations differ from each other, many methods for determination of extra-focal radiation have been investigated based on (1) direct measurement [9–11], (2) indirect measurement [12–16], and (3) Monte Carlo simulations [7, 17, 18]. However, further studies are needed for investigation of the experimental methods for the total focal radiation and more accurate modeling for them. Therefore, our purpose in this study was to develop a method for measuring the total focal radiation including focal-spot radiation and extra-focal radiation, and then estimating the focal and extra-focal radiation profiles of linear accelerators separately based on Gaussian modeling.

2 Methods and materials

2.1 Total X-ray focal radiation profile model based on Gaussian functions

The total X-ray focal radiation profile measured by a slit assembly has been modeled by double Gaussian functions representing a direct focal-spot radiation and an extra-focal radiation [9–11]. In this study, the extra-focal radiation is considered the scatter source, which is produced mainly by Compton scattering in the field-flattening filter and primary collimator [19]. However, the radiation transmitted through the slit assembly has not been taken into account in the total focal radiation profile model. Therefore, we propose a total focal radiation profile model approximated with triple Gaussian functions, which is given by

$$F(x) = G_f(x) + G_e(x) + G_t(x) + b \tag{1}$$

and

$$G_i(x) = a_i \exp\left(-\frac{1}{2}\frac{x^2}{\sigma_i^2}\right) (i = f, e, t) \tag{2}$$

where f, e, and t correspond to the focal-spot radiation, extra-focal radiation, and radiation transmitted [20] through and around the edge of the slit assembly (slit corner), respectively, a_i as well as σ_i are the peak height and width parameters of each Gaussian function, respectively, and b is the background signal. Because the peak width parameter σ_i is related to the spread of each radiation profile rather than the statistical standard deviation (SD), the parameter σ_i of a Gaussian function is called a "peak width" of the Gaussian function in this study. It is common knowledge that the full width at half maximum is $2\sqrt{2\ln 2}\,\sigma$. All parameters in Eq. 1 were determined by following two steps so that the approximate model of Eq. 1 can fit the experimental data of the total focal radiation profile obtained by a method described in the next section. In the first step, the peak width σ_f of the focal-spot radiation profile was determined by fitting of Eq. 1 with the narrow total focal radiation profile obtained by use of a 0.1-mm slit. In the second step, all other parameters in Eq 1 except the peak width σ_f of the focal-spot radiation profile, i.e., the peak heights (a_f, a_e, and a_t) and peak widths (σ_e, σ_t), were determined by fitting of Eq. 1 with the broad total focal radiation profile obtained by use of a 0.4-mm slit.

2.2 Measurement of total X-ray focal radiation profiles

The total X-ray focal radiation profiles of a linear accelerator were measured by moving a collimator-slit assembly in conjunction with a photon field p-type silicon diode. Figure 1 shows an illustration of the experimental setup for measurement of a total focal radiation profile of the linear accelerator. A megavoltage linear accelerator (Clinac 21 EX; Varian, Palo Alto, USA) producing 4-MV and 10-MV photon beams was used as the radiation source in our experiments. The irradiation field was set to 5.0 × 5.0 cm^2 at an isocenter of 100 cm. The collimator-slit assembly consisted of one to five sheets of paper (each thickness: 0.1 mm) sandwiched by two solid iron blocks [6 cm

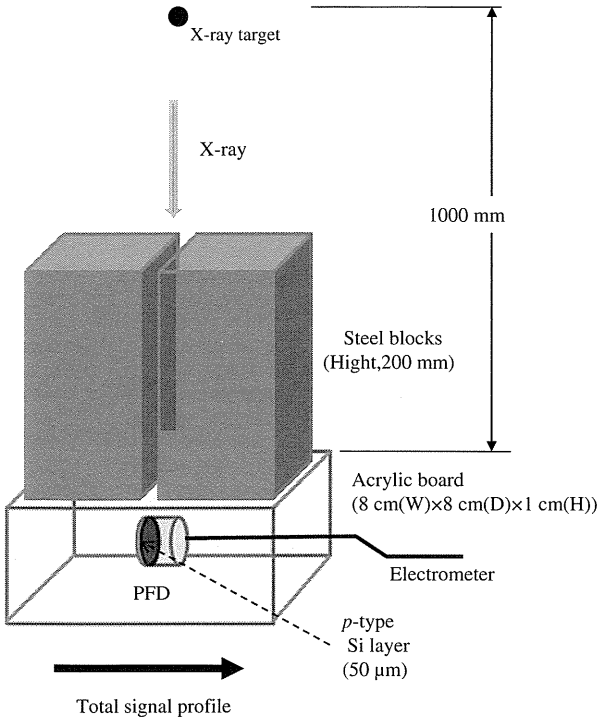

Fig. 1 Illustration of the experimental setup for measurement of total focal radiation profiles of a linear accelerator

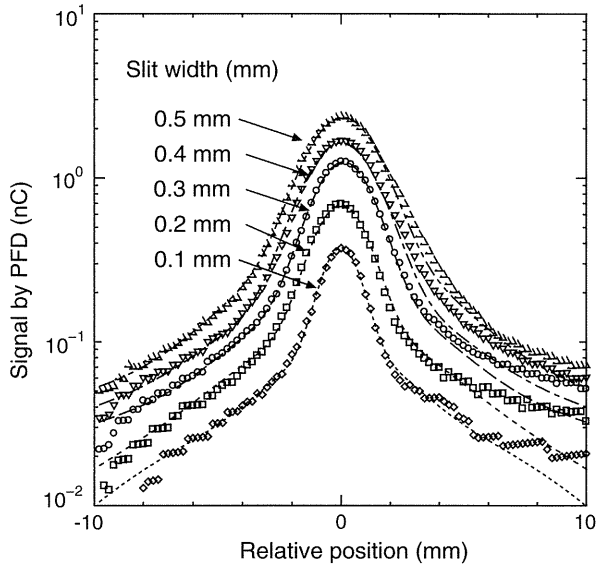

Fig. 2 Total focal radiation profiles measured for 10-MV X-rays by a slit assembly with slit widths of 0.1, 0.2, 0.3, 0.4, or 0.5 mm. The *open symbols* correspond to the signal measured by a PFD, and the *dotted lines* indicate the approximated models

(W) × 6 cm (D) × 20 cm (H), PLAT-SSB-A200-B60-T60, MISUMI, Japan], whose flatness was 200 ± 0.2 mm. The collimator-slit assembly in conjunction with a photon field detector (PFD; Scanditronix Medical AB, Uppsala, Sweden) was moved in a horizontal direction by use of a stepping motor (Suruga Seiki stepping motor controller Model D70) across the focal spot. The PFD was mounted below the center of the collimator-slit assembly. The other end of the PFD was connected to an electrometer (RAMTEC 1000 plus TOYO MEDIC, Japan). The PFD has an effective diameter of 2.0 ± 0.1 mm and a 50-μm thick *p*-type Si layer, and can be used for 1–50 MV.

For investigation of the dependence of slit width on the total focal-spot radiation profiles, the total focal radiation profiles were scanned by a slit assembly with slit widths of 0.1, 0.2, 0.3, 0.4, or 0.5 mm within ±10 mm from a beam axis with a scanning pitch of 0.2 mm for 10-MV X-rays. For determination of the Guassian parameters in Eq. 2, two types of total focal radiation profiles, i.e., narrow and broad total focal radiation profiles, were measured by use of two slit widths of 0.1 and 0.4 mm, respectively. The narrow total focal radiation profile was scanned within ±5 mm from a beam axis with a slit width of 0.1 mm and a scanning pitch of 0.1 mm, but a 1-mm pitch outside ±5 mm. The broad total focal radiation profile was measured within ±15 mm from a beam axis with a slit width of 0.4 mm and a scanning pitch of 0.2 mm.

Because both profiles contained the background signal, the background signal was subtracted from the measured profiles for determination of the net profiles, which were used in this study. We considered the background signal as diode dark signal and very weak radiation transmitted through the iron block used for the slit assembly, which would not include the radiation transmitted through and around the edge of the slit assembly. The background signal was measured by moving an iron block without a slit under the same conditions as those of the profile measurement at a scanning pitch of 1 mm.

3 Results

Figure 2 shows the total focal radiation profiles measured by a slit assembly with slit widths of 0.1, 0.2, 0.3, 0.4, or 0.5 mm for 10-MV X-rays. The approximate models indicated by dotted lines were fitted with the measured signal. However, the tail data in the radiation profile obtained by the 0.1-mm slit fluctuated greatly. Figure 3 shows the relationship between the slit width and the average fluctuation of the measured data around the tail. The average fluctuation of the measured data was defined by the average difference between the measured data and the approximate model around the tail (−9.8 to −7.2 mm, 7.2 to 9.8 mm). The data measured by the 0.1-mm slit were the most unstable because of the very small number of photons. Therefore, this result suggested that the

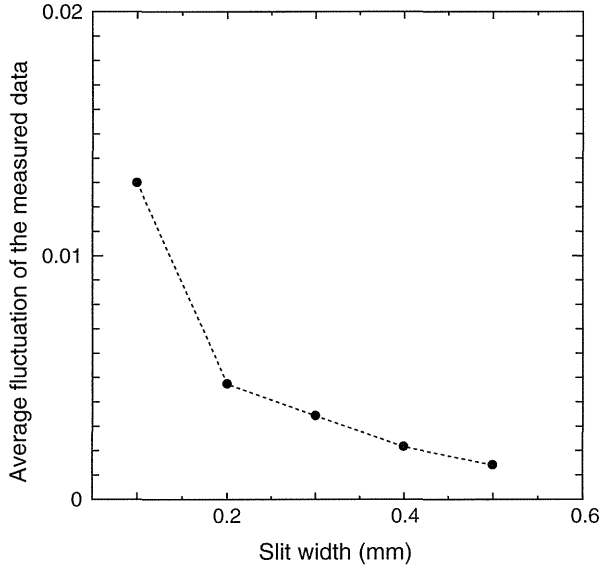

Fig. 3 Relationship between the slit width and the average fluctuation of the measured data around tail outside ±2 standard deviations

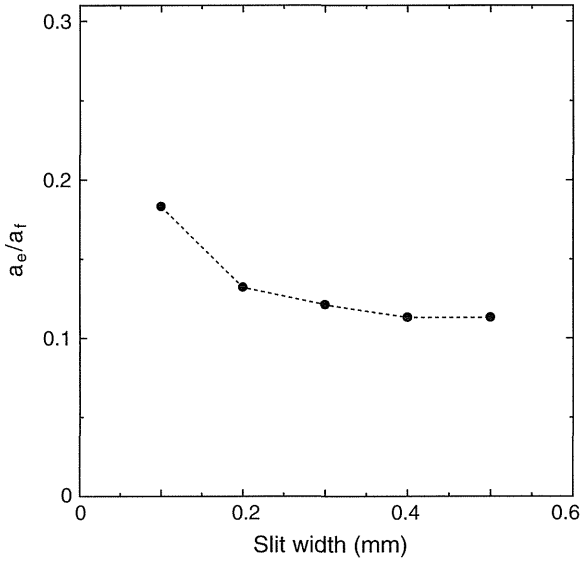

Fig. 4 Relationship between the slit width and the ratio (a_e/a_f) of the Gaussian height of the extra-focal radiation (a_e) to that of the focal-spot radiation (a_f) in the approximated model expressed by Eq. 2

parameters of the extra-focal radiation profile and the transmitted radiation would be considered to be inaccurate when the parameters were determined for such inaccurate tail data. Consequently, we decided to use the 0.1-mm slit only for determination of the peak width σ_f of the focal-spot radiation.

Figure 4 shows the relationship between the slit width and the ratio (a_e/a_f) of the Gaussian height of the extra-focal radiation (a_e) to that of the focal-spot radiation (a_f) in the approximate model expressed by Eq. 2. Figure 5 shows the relationship between the slit width and the peak widths of the focal-spot (σ_f), extra-focal (σ_e), and transmitted radiation (σ_t) profiles expressed by the Gaussian function in Eq. 2. According to Fig. 4, slits with a width larger than 0.4 mm would be better, because the ratio (a_e/a_f) did not change from the 0.4-mm width to the 0.5-mm width. In addition, because the extra-focal radiation and transmitted radiation contribute to the tail region of the total radiation profile, we need stable experimental data in the tail region, which was fitted by the approximate model. The data fluctuation around the tail region of the total focal radiation profile shown in Fig. 3 seems to be small for slit widths larger than 0.4 mm. Furthermore, as shown in Fig. 5, the peak width of the extra-focal radiation profile seems to become constant for slit widths larger than 0.4 mm. Therefore, we considered that the 0.4-mm slit width would be proper for determination of the peak heights and peak widths for the extra-focal radiation and transmitted radiation profiles.

Figure 6 shows the measured signal (solid circle) and the approximate model (solid line) of the narrow total

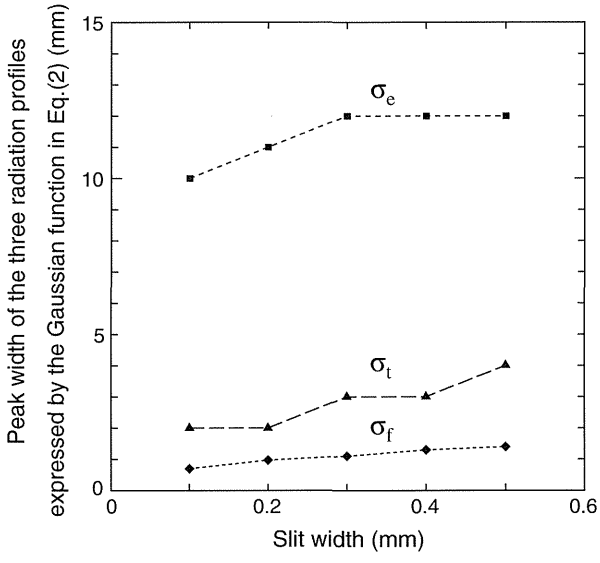

Fig. 5 Relationship between the slit width and the peak widths of focal-spot (σ_f), extra-focal (σ_e), and transmitted radiation (σ_t) profiles expressed by the Gaussian function in Eq. 2

X-ray focal radiation profile with use of a 0.1-mm slit obtained for 4-MV and 10-MV X-ray beams. The measured data fluctuate on the tail of the total X-ray focal radiation profile outside ±5 mm, because the number of photons decreases on the tail of the radiation profile obtained with a 0.1-mm narrow slit.

Figure 7 shows the relative error in the total focal radiation profile within ±5 mm between the measured

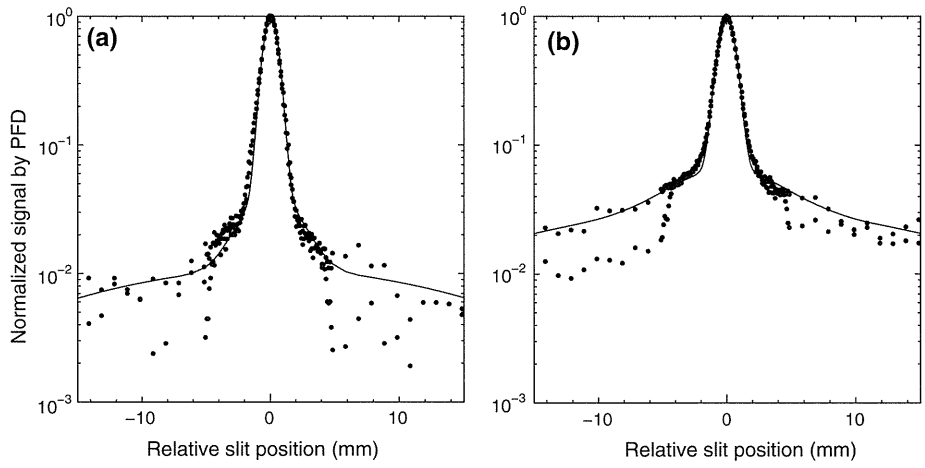

Fig. 6 Measured signal (*solid circle*) and the approximated model (*solid line*) of the narrow total X-ray focal radiation profile with a 0.1-mm slit obtained for (**a**) 4-MV and (**b**) 10-MV X-ray beams

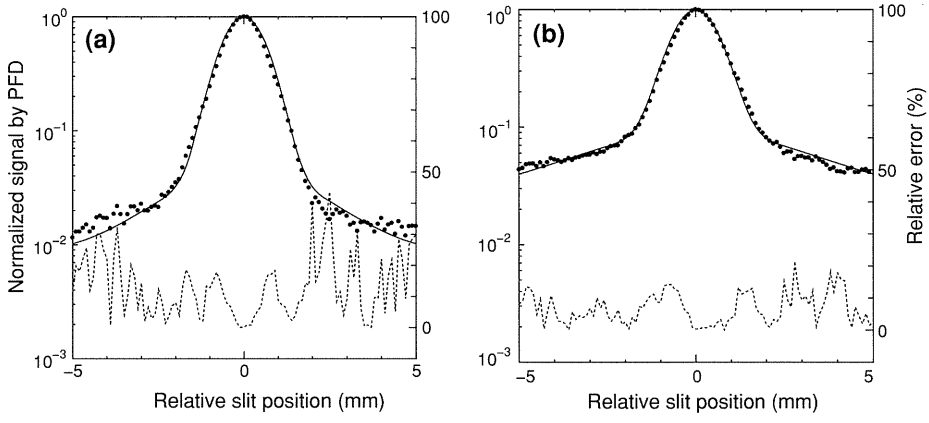

Fig. 7 Relative error (*dotted line*) in the total focal radiation profile within ±5 mm between the measured signal and approximated model for a 0.1-mm slit obtained for (**a**) 4-MV and (**b**) 10-MV X-ray beams. The *solid circles* and *solid lines* indicate the measured signal and the approximated model, respectively, which are the same data as shown in Fig. 6

signal and the approximate model for a 0.1-mm slit, obtained for 4-MV and 10-MV X-ray beams. The solid circles and solid lines indicate the measured signal and the approximated model, respectively, which are the same data as shown in Fig. 6. The relative error (%) was defined by the measured value minus the approximated value divided by the measured value. The relative error was smaller than 50% for 4 MV, but was 20% for 10 MV.

Figure 8 shows the measured signal (solid circle) and the approximate model (solid line) of the broad total focal radiation profile measured and approximated by the proposed method with a slit width of 0.4 mm for 4-MV and 10-MV X-rays. Figure 8 also shows the relative error in the total focal radiation profile between the measured signal and the approximated model. The relative errors for 4 and 10 MV were smaller than 20 and 10%, respectively.

Table 1 shows the parameters in Gaussian models, which were obtained by the proposed method, approximated for total focal radiation profiles for 4 and 10 MV. As a result, the ratios of the Gaussian peak value of the extra-focal radiation to that of the focal spot for 4 and 10 MV were 0.077 and 0.159, respectively. The peak widths of the focal-spot and extra-focal radiations were 0.57 and 25.0 mm for 4 MV, respectively, and 0.60 and 22.0 mm for 10 MV, respectively.

4 Discussion

We have developed an experimental method for measuring the total focal radiation distribution including focal-spot radiation and extra-focal radiation, and then estimating the focal and extra-focal radiation profiles of linear accelerators separately based on a triple Gaussian model. Sham et al. [11] published a study similar to ours, and they proposed an experimental method for measurement of the total focal radiation profile using a slit width of 0.3 mm, where the profiles were approximated by two Gaussian functions. On the other hand, we used an approximate model of triple Gaussian functions, taking into account radiation transmitted through and around the edge of the slit assembly. Furthermore, we proposed a two-step method

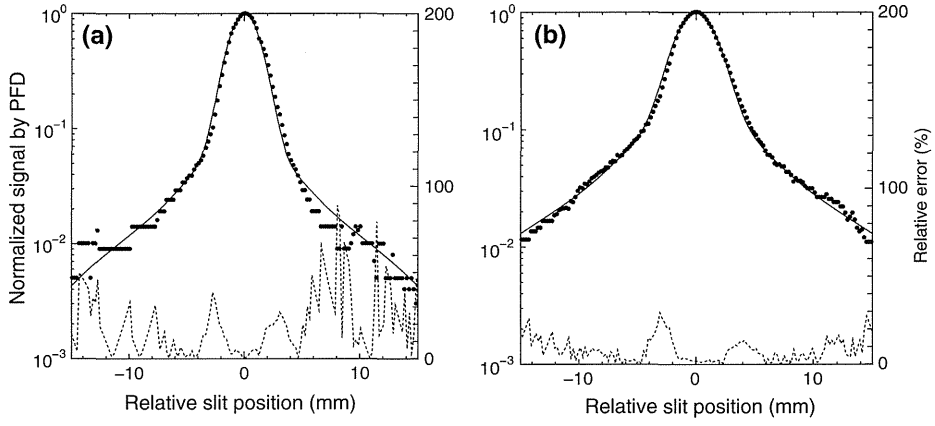

Fig. 8 Measured signal (*solid circle*) and the approximated model (*solid line*) of the total broad X-ray focal radiation profile with a 0.4-mm slit obtained for (**a**) 4-MV and (**b**) 10-MV X-ray beams. This figure also shows the relative error (*dotted line*) in the total focal radiation profile within ±15 mm between the measured signal and the approximated model for a 0.4-mm slit obtained for (**a**) 4-MV and (**b**) 10-MV X-ray beams

Table 1 Parameters in a Gaussian model approximating total focal radiation profiles obtained by the proposed method

X-ray energy (MV)	Triple-Gaussian model parameters						
	a_f	σ_f (mm)	a_e	σ_e (mm)	a_t	σ_t (mm)	a_e/a_f
4	3.00	0.57	0.23	25.0	0.65	4.20	0.077
10	3.47	0.60	0.55	22.0	1.23	6.10	0.159

Table 2 Peak width: comparisons of the focal-spot radiation profile and extra-focal radiation profile between our study and other studies

	X-ray energy (MV)	σ_f (mm)	σ_e (mm)	a_e/a_f
Jaffray et al. [9]	6	0.30–1.45	0.93	0.020
Sharpe et al. [10]	6	0.43–0.85	–	0.120
Sham et al. [11]	6	0.65	9.93	0.162
Our study	4, 10	0.57, 0.60	25.0, 22.0	0.077, 0.159

for determination of Gaussian parameters of the focal-spot radiation profile and the extra-focal radiation profile using narrow and broad total focal radiation profiles measured by slits with two widths.

Gaussian models of the focal-spot radiation profile and the extra-focal radiation profile based on experimental data are useful and necessary for Monte Carlo simulations for estimating accurate dose distributions at penumbral area [3]. If the focal radiation profiles were incorrect, the dose profiles at the penumbral area obtained by the Monte Carlo simulation could not be consistent with measured data. In particular, the discrepancy could become large in the SBRT, where steep dose gradients outside a tumor should be required in a small irradiation field.

Table 2 shows a comparison of the peak widths of the focal-spot radiation profile and the extra-focal radiation profile between our study and other studies based on experimental methods. Jaffray et al. [9] obtained nine focal-spot radiation profiles of linear accelerators using a computed tomography reconstruction technique. The peak width of the focal-spot radiation profile ranged from 0.30 to 1.45 mm, the peak width of the extra-focal radiation profile was 0.93 mm, and the a_e/a_f ratio was 0.02. Sharpe et al. [10] measured the extra-focal radiation for a 6-MV X-ray beam, where the peak widths of the focal-spot radiation profiles were from 0.43 to 0.85 mm, and the a_e/a_f ratio was approximately 12%. Sham et al. [11] evaluated the total focal radiation profiles using a simplified moving slit technique in conjunction with a diode detector for a megavoltage 6-MV linac. They reported that the peak widths of the focal-spot and extra-focal radiation profiles were 0.65 and 9.93 mm, respectively, and the a_e/a_f ratio was 0.162. On the other hand, the a_e/a_f ratios obtained based on Monte Carlo simulation ranged from 0.065 to 0.088 according to Mohan et al. [18], and from 0.03 to 0.09 according to Chaney et al. [17]. As a result, our data on the focal-spot radiation profile and the a_e/a_f ratio were close to the data of Sharpe et al. except for the peak width of the extra-focal radiation profiles. Because few data on the peak width of the extra-focal radiation profiles were reported in past studies, we should continue to investigate the methods for measurement of the extra-focal radiation profiles.

5 Conclusions

We have proposed an experimental method for estimating focal-spot and extra-focal radiation profiles of linear accelerators based on triple Gaussian functions. As a result, the ratios of the Gaussian peak height of the extra-focal radiation to that of the direct focal spot, which were measured by this proposed method, were close to previous results. Therefore, we conclude that the proposed focal-profile model based on the triple Gaussian functions may

be feasible for estimating the X-ray focal-spot and extra-focal radiation profiles.

Acknowledgments The authors thank Mr. Kazuharu Nishitani and Mr. Tokuhiro Hayashi for assistance in measurements of the total focal radiation profile.

References

1. Martin A, Gaya A. Stereotactic body radiotherapy: a review. Clin Oncol. 2010;22(3):157–72.
2. Nagata Y, Matsuo Y, Takayama K, Norihisa Y, Mizowaki T, Mitsumori M, et al. Current status of stereotactic body radiotherapy for lung cancer. Int J Clin Oncol. 2007;12(1):3–7.
3. Wang LLW, Leszczynski K. Estimation of the focal size and shape for a medical linear accelerator by Monte Carlo simulation. Med Phys. 2007;34(2):485–8.
4. Mackie TR, Scrimger JW, Battista JJ. A convolution method of calculating dose for 15-MV X rays. Med Phys. 1985;12(2): 188–96.
5. Boyer AL, Mok EC. Calculation of photon dose distributions in an inhomogeneous medium using convolutions. Med Phys. 1986;13:503–9.
6. Ahnesjö A. Collapsed cone convolution of radiant energy for photon dose calculation in heterogeneous media. Med Phys. 1989; 16(4):577–92.
7. Liu HH, Mackie TR, McCullough EC. Correcting kernel tilting and hardening in convolution/superposition dose calculations for clinical divergent and polychromatic photon beams. Med Phys. 1997;24(11):1729–41.
8. Battista JJ, Sharpe MB. True three-dimensional dose computations for megavoltage X-ray therapy: a role for the superposition principle. Australas Phys Eng Sci Med. 1992;15(4):159–78.
9. Jaffray DA, Battista JJ, Fenster A, Munro P. X-ray source of medical liner accelerators: focal and extra-focal radiation. Med Phys. 1993;20(5):1417–27.
10. Sharpe MB, Jaffray DA, Battista JJ, Munro P. Extrafocal radiation: a unified approach to the prediction of beam penumbra and output factors for megavoltage X-ray beams. Med Phys. 1995; 22(12):2065–74.
11. Sham E, Seuntjens J, Devic S, Podgorsak EB. Influence of focal spot on characteristics of very small diameter radiosurgical beams. Med Phys. 2008;35(7):3317–30.
12. Ahnesjö A, Knöös T. Application of the convolution method for calculation of output factors for therapy photon beams. Med Phys. 1992;19(2):295–301.
13. Ahnesjö A. Analytic modeling of photon scatter from flattening filters in photon therapy beams. Med Phys. 1994;21(8):1227–35.
14. Zhu TC, Bjarngard BE. The head-scatter factor for small field sizes. Med Phys. 1994;21(1):65–8.
15. Das IJ, Ding GX, Ahnesjö A. Small fields : nonequilibrium radiation dosimetry. Med Phys. 2008;35(1):206–15.
16. Scott AJD, Nahum AE, Fenwick JD. Monte Carlo modeling of small photon fields: quantifying the impact of focal spot size on source occlusion and output factors, and exploring mini phantom design for small-field measurements. Med Phys. 2009;36(7): 3132–44.
17. Chaney EL, Cullip TJ, Gabriel TA. A Monte Carlo study of accelerator head scatter. Med Phys. 1994;21(9):1383–90.
18. Mohan R, Chui C, Lidofsky L. Energy and angular distributions of photons from medical linear accelerators. Med Phys. 1985; 12(1):592–7.
19. DeLuca P, Jones D, Gahbauer R. Prescribing, recording, and reporting photon-beam intensity-modulated radiation therapy (IMRT). ICRU report 83. 2010;10(1):60–6
20. Sawant A, Antonuk L, El-Mohri Y. Slit design for efficient and accurate MTF measurement at megavoltage X-ray energies. Med Phys. 2007;34(5):1535–45.

II. 臨　　床

前立腺癌の治療
放射線療法　外照射

外照射療法の現状と展望

Trends and future of external radiotherapy for prostate cancer

中村和正[1]　　佐々木智成[2]

Key words：外照射，強度変調放射線治療，画像誘導放射線治療，寡分割照射，hypofractionation

はじめに

外照射を含めた放射線治療は，近年急速に進歩している．我が国においても，三次元原体放射線治療(three-dimensional conformal radiotherapy: 3DCRT)，強度変調放射線治療(intensity-modulated radiotherapy: IMRT)，画像誘導放射線治療(image-guided radiotherapy: IGRT)などの最新の技術が実際に臨床の現場に導入されてきている．また，線量増加の有用性などに関する臨床試験の結果が次々と明らかとなり，臨床現場へフィードバックされることにより，前立腺癌に対する放射線治療の照射法，線量などは急速に変化しつつある．

本稿では，外照射の現状とその将来展望について解説する．

1. 外照射の現状

外照射の技術的な進歩は，悪性腫瘍に対する放射線治療の成績の向上に大きく貢献してきた．特に，前立腺癌に対しては，直腸線量を低減することで，更に多くの線量を照射できるため，積極的に最新技術が導入されている．このような状況で，前立腺癌の放射線治療が我が国においてどのように行われており，どのように変化しているかを恒常的にモニタすることは非常に重要である．これらを明らかにする研究の一つが，医療実態調査研究(Patterns of Care Study: PCS)である．

PCSは，米国で開発された臨床的精度管理QAの手法の一つで，structure，process，outcomeの分析を行うものである[1]．我が国には1996年より本格的に導入され，厚生労働省がん研究助成金の援助を受け，研究者がランダムに選択された全国の放射線治療施設を訪問し，ランダムに抽出された各疾患の治療のプロセス，成績などを調査してきた[2]．前立腺癌に対しては，1996-98年，1999-2001年，2003-05年に放射線治療が行われた遠隔転移または重複癌を伴わない前立腺癌症例が調査され[3,4]，計177施設より，根治的外照射例852例，術後照射例278例，内分泌療法抵抗・再燃例189例，その他104例(組織内照射施行例84例含む)，合計1,423例が集積されている．

根治的外照射852例についてみると[5]，T因子は，T1: 16.6%，T2: 38.7%，T3: 38.2%，T4: 6.5%であった．また，リンパ節転移例は6.5%であった．Gleasonスコアは，2-6: 35.5%，7: 31.8%，8-10: 32.7%であった．全治療前のPSA(prostate specific antigen)値は，<10ng/mL:

[1]Katsumasa Nakamura: Department of Radiology, Kyushu University Hospital at Beppu　九州大学病院別府先進医療センター 放射線科　[2]Tomonari Sasaki: Department of Radiology, National Kyushu Cancer Center　九州がんセンター 放射線治療部

0047-1852/11/¥60/頁/JCOPY

29.8％，10–19.9 ng/mL: 24.4％，≧20 ng/mL: 45.9％であった．経年的変化としては，T1–2の割合は1996–98年34.6％から，2003–05年64.6％と上昇しており，PSA値の中央値は，1996–98年22 ng/mLから2003–05年14.9 ng/mLと低下していた．すなわち，放射線治療にて治療される早期前立腺癌症例が増加していることがわかる．内分泌療法施行割合は84.9％と，多くの症例に内分泌療法が併用されていた．放射線治療に関しては，58.0％に3DCRTが施行されていたが，その割合は，1996–98年49.1％から2003–05年66.4％と上昇している．照射線量の中央値は，1996–98年65 Gyから2003–05年70 Gyと上昇しており，経年的に，より高精度な照射方法にて高い線量が投与される傾向にあることを示している．

このように，PCSは，放射線治療の構造面，診療過程を全国規模で調査し，解析することによって，診療上の変化に加えて，照射野設定，線量分割などを含めた診療の質を同時にモニタでき，日本の放射線治療の質の向上に寄与してきた．米国では，このような研究はThe Quality Research in Radiation Oncology(QRRO)として継続されており，米国での放射線治療の質の維持・向上に重要な役割を果たしている．今後，我が国での前立腺癌の放射線治療では，IMRTやIGRTなどの新しい技術が更に普及してくるものと思われる．また，粒子線治療により治療される前立腺癌症例も増加するであろう．このように，今後とも急激に変化していく放射線治療の実態を調査し，その診療の質を評価する研究の重要性は更に増すものと考えられる．

2. 画像誘導放射線治療

放射線治療のターゲットとなる前立腺の位置は，毎回の治療ごとに変動することが知られている．これは，セットアップエラーに加えて，直腸，膀胱容量などによっても前立腺の位置が影響されることによる．もし，この治療ごとの位置変動を小さくすることができれば，より小さい照射野で照射でき，有害事象を低減化できる可能性がある．

前立腺の位置の不確定要素を低減する方法としては，金属マーカーを前立腺周囲に挿入し，治療直前にX線透視などでマーカーの位置を確認する方法，治療装置に連携した超音波装置やCTなどにより位置確認を行う方法などがある．このような方法は，画像誘導放射線治療(image-guided radiotherapy: IGRT)と呼ばれ，近年急速に普及しつつある．

我が国において，IGRTが前立腺癌の外照射においてどのように使用されているか，不明であった．そこで，厚生労働省科学研究費による‘放射線治療期間の短縮による治療法の有効性と安全性に関する研究’では，IGRT，IMRTの実施状況に対してアンケートを行った．平成22年に全国大学病院/がんセンター，都道府県がん診療連携拠点病院を含む主要139施設にアンケートを送付し，117施設(84.2％)より回答を得た．IMRT実施施設は67施設(57.3％)，IGRT実施施設は71施設(60.7％)であった．しかし，IMRT未導入施設のうち75％，IGRT未導入施設のうち65％が3年以内に導入予定としている．すなわち，数年以内に多くの施設でIMRT，IGRTが行われるようになると考えられる．照射については，93.0％の施設が週5回法，86.6％の施設が1回2 Gyにて治療を行っていた．投与線量は，**図1**に示すように，3DCRTでは中央値70 Gy，IMRTでは中央値76 Gyであり，明らかにIMRTにて高線量が投与されていた．IGRTについては，kVCT，MVCT，透視装置，超音波装置，金属マーカーなど，様々な手法で行われており，IMRTなどの高精度治療が実施される場合にはほぼ全例に，ほぼ毎日IGRTでの位置確認が行われていた．位置確認については，47.1％が骨情報，40.0％が前立腺などの軟部組織，12.9％が金属マーカーでの位置合わせであった．

このアンケートからもわかるように，少なくとも大規模施設においては，数年以内にIMRT，IGRTが広く普及すると予想され，今後の前立腺癌の外照射の成績向上が期待される．

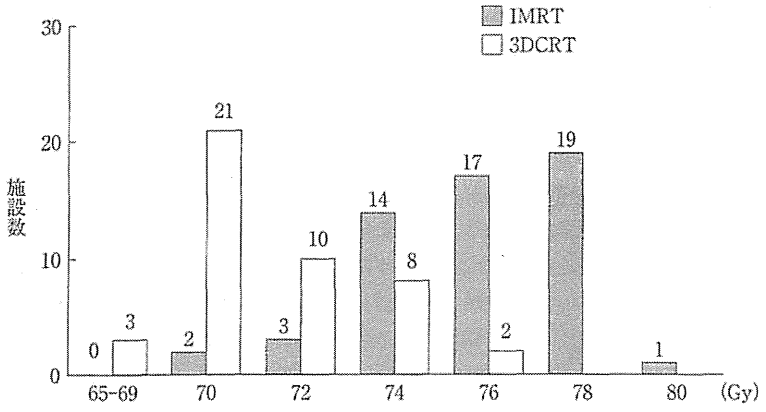

図1 治療法別の前立腺に対する総線量の分布
1回線量1.8–2.0 Gyにて治療している全国100施設を対象とした.
IMRT: 強度変調放射線治療, 3DCRT: 三次元原体放射線治療.

3. 寡分割照射

上述のように，IGRTが普及することのメリットの一つは，毎回の治療ごとのセットアップエラーなどによる位置変動を小さくすることにより，治療成績向上に貢献することである．実は，もう一つの利点として，1回線量を増加させ，治療回数を減らす(寡分割照射，hypofractionation)ことが可能となる点があげられる．

放射線に対する感受性の指標としてα/β比が知られており，通常の悪性腫瘍は10程度，直腸などの正常組織では3程度とされており，1回線量を大きくすると，α/β比の小さい正常組織では有害事象の可能性が高くなり，腫瘍のコントロール率向上のメリットよりもマイナス面の方が大きいとされている．しかし，増殖速度の遅い前立腺癌のα/β比は非常に小さく，周囲の正常組織である直腸や尿道などのα/β比よりも小さいと推測されている[6]．もしこの予想が正しければ，1回線量の増加により，有害事象の発生率は変えずに治療成績を向上させることができるかもしれない．

通常分割(1回線量1.8–2 Gy)での前立腺癌に対する照射回数は37–40回程度であり，セットアップエラーや直腸容積などによる前立腺位置の変動があっても，多数回の照射により平均化されるため，それほど治療成績に影響しない．しかし，照射野のマージンが小さい場合，1回線量をより大きくし，分割回数を小さくすればするほど，前立腺の位置の不確定要素が治療成績に大きく関係してくるようになる[7]．すなわち，毎回の前立腺の位置の不確定要素を低減させるIGRTを用いることで，初めて寡分割照射を安全にかつ効果的に実現できると考えられている．

寡分割照射については，既に多くの報告がある．レトロスペクティブな報告で，大規模なものとして，Cleveland Clinicからの1回2.5 Gy, total 70 Gyの治療成績の報告がある[8]．超音波装置を使って前立腺の位置を同定してIMRTにて治療された770例の5年PSA無再発率は82％と良好であり，Grade 2以上の直腸障害，尿路系障害はそれぞれ4.5％，5.2％と通常分割法と同程度であったとしている．

現在，寡分割照射の有効性を確認するために，IGRTを使って，通常分割照射(1回1.8–2 Gy)と寡分割照射(1回2.5–3 Gy程度)との大規模なランダム化比較試験が幾つか実施されており[9]，これらの結果によっては，寡分割照射がスタンダードの一つとなる可能性を秘めている．

前立腺癌に定位的に放射線治療を行い，更に少ない回数で，1回大線量を投与する試みもある．Bolzicco ら[10]は，低～中リスク前立腺癌45例に対して，Cyberknifeにより定位的に35

Gy/7分割(1回7Gy)を照射し，20カ月の経過観察期間にて，Grade 2以上の晩期有害事象は4.4％と良好であったと報告している．しかし，このような大線量，少数分割の長期成績は不明であり，いまだ研究的な治療法であることに注意しなければならない．

おわりに

いままで述べてきたように，IMRT，IGRTが前立腺癌の外照射に急速に応用されるようになっており，より有害事象の発生を抑えた治療が可能となっている．更に，それらの技術的な進歩を背景として，寡分割照射の有用性が世界中で検討されている．外照射の欠点は，7-8週間程度と治療期間が長期にわたる点であったが，もし寡分割照射の大規模比較試験の結果が明らかとなれば，より短期間で外照射が実施可能となるかもしれない．今後の研究成果が期待される．

文献

1) Hanks GE, et al: Patterns of Care Studies—Past, Present, and Future—. Semin Radiat Oncol 7: 97-100, 1997.
2) 手島昭樹：放射線腫瘍学における医療実態調査研究—わが国における臨床施行の成果と意義，将来目標—．日放線腫瘍会誌 12: 1-12, 2000.
3) Nakamura K, et al: Trends in the practice of radiotherapy for localized prostate cancer in Japan: a preliminary patterns of care study report. Jpn J Clin Oncol 33: 527-532, 2003.
4) Ogawa K, et al: Radical External Beam Radiotherapy for Clinically Localized Prostate Cancer in Japan: Changing Trends in the Patterns of Care Process Survey. Int J Radiat Oncol Biol Phys, 2010. Oct 13. [Epub ahead of print]
5) 中村和正：外照射—3DCRT，IMRT，陽子・重粒子線．限局性(T1，T2)前立腺癌の治療．第36回尿路悪性腫瘍研究会記録，p54-58, 2010.
6) Williams SG, et al: Use of individual fraction size data from 3756 patients to directly determine the alpha/beta ratio of prostate cancer. Int J Radiat Oncol Biol Phys 68: 24-33, 2007.
7) Song WY, et al: Evaluation of image-guided radiation therapy(IGRT) technologies and their impact on the outcomes of hypofractionated prostate cancer treatments: a radiobiologic analysis. Int J Radiat Oncol Biol Phys 64: 289-300, 2006.
8) Kupelian PA, et al: Hypofractionated intensity-modulated radiotherapy(70Gy at 2.5Gy per fraction) for localized prostate cancer: Cleveland Clinic experience. Int J Radiat Oncol Biol Phys 68: 1424-1430, 2007.
9) Miles EF, Lee WR: Hypofractionation for prostate cancer: a critical review. Semin Radiat Oncol 18: 41-47, 2008.
10) Bolzicco G, et al: Image-guided stereotactic body radiation therapy for clinically localized prostate cancer: preliminary clinical results. Technol Cancer Res Treat 9: 473-477, 2010.

JJCO Japanese Journal of Clinical Oncology

Jpn J Clin Oncol 2011;41(9)1127–1131
doi:10.1093/jjco/hyr112
Advance Access Publication 10 August 2011

Quantification of Cold Spots Caused by Geometrical Uncertainty in Field-in-field Techniques for Whole Breast Radiotherapy

Naoki Nakamura[1,*], Shogo Hatanaka[1], Naoto Shikama[2], Keiko Akahane[1] and Kenji Sekiguchi[1]

[1]Department of Radiation Oncology, St Luke's International Hospital, Tokyo and [2]Department of Radiation Oncology, Saitama Medical University Hospital, Hidaka, Japan

*For reprints and all correspondence: Naoki Nakamura, Department of Radiation Oncology, St Luke's International Hospital, 9-1, Akashicho, Chuoh-ku, Tokyo 104-8560, Japan. E-mail: naokinak@luke.or.jp

Received May 20, 2011; accepted July 8, 2011

Objective: To quantify the cold spot under geometrical uncertainties in field-in-field techniques for whole breast radiotherapy.
Methods: Ten consecutive patients from both the left- and right-sided treatment site groups who received whole breast radiotherapy with the field-in-field technique were included. Virtual plans were made with moving isocenters to the posterior direction having two amplitudes (5 and 10 mm) and prescribing the same monitor unit as the original plan (FIF_5 and FIF_10). The planning target volume for evaluation was defined by subtracting the areas within 5 mm from the skin and within 5 mm from the lung from the whole breast. The differences in V90, V95 and D98 of planning target volume for evaluation were measured between the original and virtual plans. As a reference, the same measurements were taken for the wedge techniques (Wedge_5 and Wedge_10).
Results: The differences in V95 were −0.2% on FIF_5, −1.7% on FIF_10, −0.5% on Wedge_5 and −1.5% on Wedge_10. The differences in V90 were −0.02% on FIF_5, −0.3% on FIF_10, −0.05% on Wedge_5 and −0.1% on Wedge_10. The differences in D98 were 0 Gy on FIF_5, −0.1 Gy on FIF_10, −0.2 Gy on Wedge_5 and −0.4 Gy on Wedge_10. The differences in D98 between the original plans and virtual scenarios for field-in-field techniques were significantly smaller than those for wedge techniques, but there were no statically significant differences in V90 and V95.
Conclusions: The quantity of the cold spots caused by the geometrical uncertainties in field-in-field techniques was similar to that for the wedge techniques and was acceptable.

Key words: breast cancer – radiotherapy – whole breast radiotherapy – field-in-field technique – geometrical uncertainty

INTRODUCTION

Whole breast radiotherapy has been widely used after breast-conserving surgery to prevent local recurrence in patients with early breast cancer. A tangential parallel-opposed technique is used for whole breast radiotherapy. Achieving acceptable dose homogeneity across the whole breast volume is difficult because of the continuous change in breast shape across multiple planes and the effect of the lung tissues that are included in the irradiated volume (1, 2).

Several groups have reported that the field-in-field (FIF) technique can reduce dose inhomogeneity in whole breast radiotherapy (3–7). FIF is a forward planning intensity modulating technique. Fields are created using multileaf collimator (MLC) leaves such that the leaves are strategically placed in areas where the dose to the breast is considerably higher than the prescription dose, otherwise known as hot spots (7). However, geometrical uncertainties arising from set-up errors and respiratory motion are not considered in this

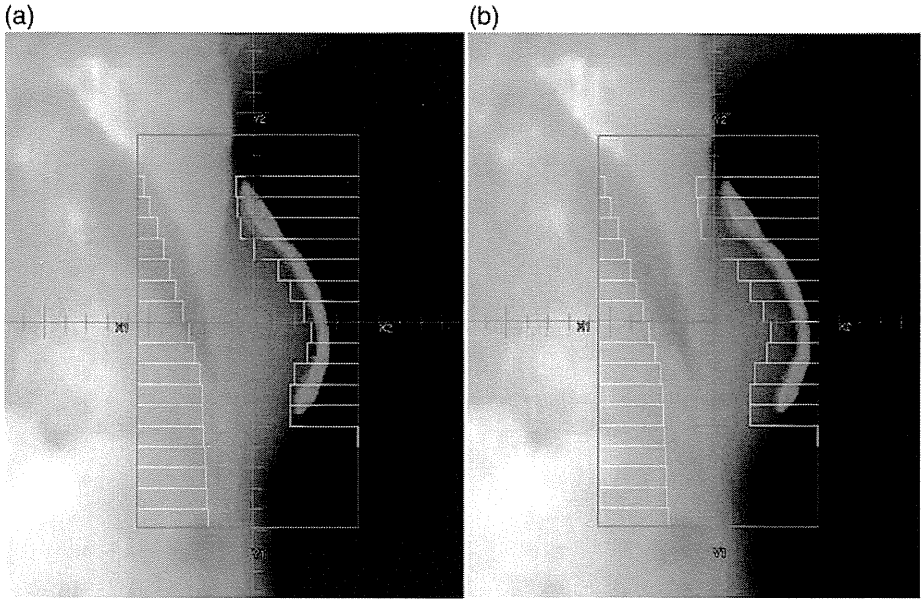

Figure 1. (a) An example of a reduction field to eliminate the hot spots. (b) A virtual field tilted to the posterior direction by 1 cm. In each figure, 107% isodose cloud is shown in blue.

strategy. If the MLC leaves are tilted to the posterior direction because of the geometrical uncertainties, cold spots where the dose to the breast is considerably lower than the prescription dose may arise.

We evaluated the quantities of cold spots caused by geometrical uncertainties in FIF techniques for whole breast radiotherapy compared with wedge plans.

PATIENTS AND METHODS

Ten consecutive patients from both the left- and right-sided treatment site groups who received whole breast radiotherapy with the FIF technique at St Luke's International Hospital were included in this study. Computed tomographic scans were performed with a LightSpeed RT16 (GE Healthcare) helical scanner and 5 mm slice thickness without breath holding. All patients were treated with 4 MV X-ray. All patients were treated with four fields, two of which were reduction fields to eliminate hot spots where the doses are higher than 107–110% of the prescription dose (Fig. 1). The treatment machine was CLINAC21EX (Varian) which has 1 cm thick MLCs. The treatment planning system (TPS) was Pinnacle ver. 8.0 m (Phillips).

We have in-house regulations to ensure the accuracy of the TPS when we use FIF techniques: do not put MLC leaves within 1 cm from the reference point, the minimum monitor unit (MU) in each field is 5, do not make any part of the field narrower than 2 cm, and the proportion of field blocked by MLC leaves must be $<50\%$.

Virtual plans were made on the TPS by moving isocenters to the posterior direction with two amplitudes (5 and 10 mm) and prescribing the same MU as in the original plan (FIF_5 and FIF_10) (Fig. 1). The planning target volume for evaluation (PTV_EV) was defined by subtracting the areas within 5 mm from the skin and within 5 mm from the lung from the whole breast (Fig. 2). The differences in the percentages of the volume of the PTV_EV which receive more than 90 and 95% of the prescribed dose (V90 and V95) and the doses received by 98% of the PTV_EV (D98) were compared between the original and virtual plans. As a reference,

Figure 2. An example of delineation of the planning target volume for evaluation (PTV_EV), defined by subtracting the areas within 5 mm from the skin and within 5 mm from the lung from the whole breast.

Table 1. V95, V90 and D98 of the planning target volume for evaluation (PTV_EV) on field-in-field (FIF) techniques for each patient

Patient #	Monitor unit (a)	V95 (%)			V90 (%)			D98 (Gy)		
		FIF_0	FIF_5	FIF_10	FIF_0	FIF_5	FIF_10	FIF_0	FIF_5	FIF_10
R-1	237 (14)	92.2	*90.3*	*90.6*	99.3	99.3	99.9	45.8	45.8	46.0
R-2	231 (11)	93.4	96.2	95.5	100.0	100.0	100.0	46.9	47.2	47.1
R-3	234 (12)	99.5	99.6	99.6	100.0	100.0	100.0	48.3	48.4	48.4
R-4	238 (12)	99.3	99.3	99.3	100.0	100.0	100.0	48.2	48.2	48.2
R-5	233 (16)	96.4	*96.2*	*93.4*	100.0	100.0	100.0	47.3	47.3	*47.0*
R-6	227 (14)	83.2	*82.3*	*77.5*	95.4	*95.3*	*92.5*	44.1	*44.0*	*43.8*
R-7	237 (15)	98.3	*98.2*	*97.8*	100.0	100.0	100.0	47.6	47.6	*47.5*
R-8	228 (12)	91.8	*91.6*	*89.2*	99.0	99.0	99.0	45.6	45.6	*45.5*
R-9	240 (13)	88.6	*88.4*	*86.1*	98.3	98.3	*98.2*	45.2	45.2	45.2
R-10	237 (12)	95.4	95.4	*94.3*	99.9	99.9	99.9	46.6	46.6	*46.4*
L-1	232 (12)	92.1	92.2	88.0	99.9	99.9	99.9	46.0	46.2	46.0
L-2	239 (12)	72.2	*71.3*	*66.7*	94.9	*94.8*	*94.4*	44.1	44.1	*44.0*
L-3	250 (15)	87.9	87.9	*87.7*	100.0	100.0	100.0	46.2	46.2	46.2
L-4	232 (10)	99.5	99.5	99.5	100.0	100.0	100.0	48.3	48.3	48.3
L-5	240 (18)	87.0	*86.1*	*82.7*	98.3	98.3	*97.8*	45.2	45.2	*45.0*
L-6	235 (14)	89.4	*87.3*	*85.9*	99.4	*99.3*	*96.3*	45.7	*45.6*	*44.8*
L-7	238 (12)	94.9	94.9	94.9	99.9	99.9	99.9	46.8	46.9	47.0
L-8	238 (12)	97.3	97.3	97.3	99.9	99.9	99.9	47.4	47.4	*47.3*
L-9	243 (15)	92.0	*91.8*	*90.9*	99.0	99.0	99.0	45.6	45.6	45.6
L-10	232 (10)	97.4	97.5	97.4	100.0	100.0	100.0	47.4	47.5	47.4
Average	232 (13)	92.4	*92.2*	*90.7*	99.2	*99.1*	*98.8*	46.4	46.4	*46.3*

V95 (90) is the percentage of the PTV_EV that receives more than 95% (90%) of the prescribed dose; D98 is the dose received by 98% of the PTV_EV; FIF_0, FIF_5 and FIF_10 are the virtual plans for FIF techniques with moving isocenters to the posterior direction with 0 (original plan), 5 and 10 mm, respectively; numbers are shown in italics when the values are smaller than those on FIF_0.
[a]Monitor unit of the reduction fields.

virtual plans using a physical wedge with a 15° angle were made and the same measurements were taken on the same 20 patients (Wedge_5 and Wedge_10).

The calculation algorithm was CC Convolution. The grid size of the calculation matrix was 2 mm.

We used GraphPad Prism version 5 (GraphPad Software Inc.) for statistical analysis. The paired *t*-test was used to compare the results for FIF and wedge techniques. Differences were deemed significant when two-tailed *P* values were <0.05.

RESULTS

The mean total MU was 236 (range: 227–250) per 2 Gy. The mean percentage of MU of the reduction fields was 5.5% (4.3–7.5). The mean V90, V95 and D98 of the PTV_EV on FIF techniques were 99.2% (94.9–100), 92.4% (72.2–99.5) and 46.4 Gy (44.1–48.3), respectively, whereas the mean V90, V95 and D98 on wedge plans were 99.8% (97.9–100), 96.5% (82.8–100) and 47.4 Gy (45.0–49.0), respectively (Tables 1 and 2). The differences in D98 between the original plans and virtual scenarios for FIF techniques were significantly smaller than those for wedge techniques (Table 3). No statistically significant differences were observed in the differences in V90 and V95 between plans for FIF techniques and those for wedge techniques (Table 3).

DISCUSSION

To the best of our knowledge, this is the first report to focus on the dosimetric impact of geometrical uncertainties in FIF techniques for whole breast radiotherapy. Several groups have reported that geometrical uncertainties have a considerable impact on intensity-modulated radiation therapy (IMRT) dose distributions (8–11). Although the FIF technique is a kind of

Table 2. V95, V90 and D98 of the PTV_EV on wedge plans for each patient

Patient #	Monitor unit	V95 (%)			V90 (%)			D98 (Gy)		
		W_0	W_5	W_10	W_0	W_5	W_10	W_0	W_5	W_10
R-1	322	96.1	96.4	96.1	99.9	100.0	100.0	46.6	46.8	46.8
R-2	316	97.4	*96.7*	*95.2*	100.0	100.0	100.0	47.4	*47.3*	*47.1*
R-3	318	100.0	*99.9*	*99.8*	100.0	100.0	100.0	49.0	*48.8*	*48.4*
R-4	323	99.9	99.9	99.9	100.0	100.0	100.0	49.0	*48.8*	*48.6*
R-5	317	99.4	*98.8*	*97.5*	100.0	100.0	100.0	48.0	*47.7*	*47.5*
R-6	310	88.1	*85.8*	*82.6*	97.9	*97.4*	*96.7*	45.0	*44.9*	*44.6*
R-7	322	99.7	99.7	*99.6*	100.0	100.0	100.0	48.5	*48.3*	*48.1*
R-8	293	96.2	*95.7*	*95.0*	100.0	100.0	100.0	46.9	*46.8*	*46.6*
R-9	326	94.8	*94.0*	*92.5*	99.6	*99.5*	*99.4*	46.3	*46.2*	*46.0*
R-10	323	98.4	*98.1*	*97.6*	100.0	100.0	100.0	47.7	*47.6*	*47.4*
L-1	316	99.1	*98.3*	*96.8*	100.0	100.0	100.0	47.9	*47.6*	*47.3*
L-2	325	82.8	*82.0*	*80.1*	98.3	*97.9*	*97.3*	45.1	*45.0*	*44.8*
L-3	340	97.3	97.7	97.6	100.0	100.0	100.0	47.4	47.5	47.5
L-4	317	99.9	99.9	*99.7*	100.0	100.0	100.0	48.9	*48.7*	*48.4*
L-5	324	92.7	*91.7*	*90.1*	99.8	*99.7*	*99.6*	46.4	*46.2*	*46.0*
L-6	321	96.3	*95.1*	*92.8*	100.0	100.0	100.0	47.2	*47.0*	*46.7*
L-7	324	99.1	*98.7*	*98.1*	100.0	100.0	100.0	47.9	*47.7*	*47.6*
L-8	322	99.2	*99.0*	*98.5*	100.0	100.0	100.0	48.1	*47.9*	*47.7*
L-9	328	95.4	*94.5*	*93.2*	100.0	100.0	100.0	46.7	*46.5*	*46.3*
L-10	314	97.4	*97.2*	*96.6*	100.0	100.0	100.0	47.4	47.4	47.4
Average	320	96.5	*96.0*	*95.0*	99.8	99.7	99.7	47.4	*47.2*	*47.0*

V95 (90) is the percentage of the PTV_EV that receives more than 95% (90%) of the prescribed dose; D98 is the dose received by 98% of the PTV_EV; Wedge_0, Wedge_5 and Wedge_10 are the virtual plans for a physical wedge, moving isocenters to the posterior direction by 0, 5 and 10 mm, respectively; numbers are shown in italics when the values are smaller than those on Wedge_0.

Table 3. The mean differences (range) of V95, V90 and D98 between original plans and virtual scenarios

	V95	V90	D98
FIF_5	−0.2% (−2.1 to +2.8)	−0.02% (−0.1 to 0)	0 Gy (−0.1 to +0.3)
Wedge_5	−0.5% (−2.3 to +0.4)	−0.05% (−0.5 to +0.1)	−0.2 Gy (−0.3 to 0.2)
P	0.28	0.3	**<0.01**
FIF_10	−1.7% (−5.7 to +2.1)	−0.3% (−3.1 to +0.6)	−0.1 Gy (−0.9 to +0.2)
Wedge_10	−1.5% (−5.5 to +0.3)	−0.1% (−1.2 to +0.1)	−0.4 Gy (−0.6 to 0.2)
P	0.76	0.38	**<0.01**

V95 (90) is the percentage of the volume of the PTV_EV which receives more than 95% (90%) of the prescribed dose; D98 is the dose that 98% of the PTV_EV receives; FIF_5 (FIF_10) is the virtual plan for FIF techniques with moving isocenters to the posterior direction with 5 (10 mm); Wedge_5 (Wedge_10) is the virtual plan for a physical wedge, moving isocenters to the posterior direction by 5 (10 mm). The bold values indicate statistically significant differences.

IMRT, our results showed that the quantity of the cold spots caused by geometrical uncertainties in FIF techniques for whole breast radiotherapy was similar to that in wedge plans. This might be partly because the proportion of the reduction fields was quite low. Most patients do not need a high MU for reduction fields, but caution might be needed when the proportion of the reduction fields is a little larger.

Several groups have reported that the FIF technique can reduce dose inhomogeneity in whole breast radiotherapy compared with that using physical wedge techniques (3–7).

An additional benefit of using the FIF technique is that FIF techniques can reduce MU and dose in the contralateral breast. Lee et al. (3) have reported that the volumes in the contralateral breast that receive more than 2 Gy with a prescription dose of 50.4 Gy were 0.3% for FIF techniques, but 2.0% for physical wedge techniques ($P < 0.01$). By using the FIF techniques, the incidence of radiation-induced contralateral breast cancer might be reduced.

The possible disadvantage of using the FIF techniques is that FIF techniques may increase the uncertainties of dose calculation on the TPS. If we use fields that are too small or too irregular as the reduction fields, the TPS may not calculate the MU and the dose distributions accurately. Furthermore, if we prescribe MU that is too small, the output from the linear accelerator may become unstable. In such cases, dosimetric verification should be done for each plan. For this reason, we regulate the in-house protocol as described in the Patients and Methods section to ensure the accuracy of the TPS when we use FIF techniques in order to eliminate the necessity of dosimetric verification for individual plans.

A limitation of this study is that it evaluated a small series of patients and does not have sufficient statistical power to recognize potential differences in V90 and V95 between plans for FIF techniques and those for wedge techniques. Nevertheless, the outcomes of this study offer some guidance to clinicians in an area where data are lacking and show that the quantity of cold spots caused by geometrical uncertainties in FIF techniques is similar to that using wedge techniques.

In conclusion, the quantity of cold spots caused by geometrical uncertainties in FIF techniques for whole breast radiotherapy was similar to that on for the wedge techniques and was acceptable.

Conflict of interest statement

None declared.

References

1. Aref A, Thornton D, Youssef E, He T, Tekyi-Mensah S, Denton L, et al. Dosimetric improvements following 3D planning of tangential breast irradiation. *Int J Radiat Oncol Biol Phys* 2000;48:1569–74.
2. Buchholz TA, Gurgoze E, Bice WS, Prestidge BR. Dosimetric analysis of intact breast irradiation in off-axis planes. *Int J Radiat Oncol Biol Phys* 1997;39:261–7.
3. Lee JW, Hong S, Choi KS, Kim YL, Park BM, Chung JB, et al. Performance evaluation of field-in-field technique for tangential breast irradiation. *Jpn J Clin Oncol* 2008;38:158–63.
4. Chang SX, Deschesne KM, Cullip TJ, Parker SA, Earnhart J. A comparison of different intensity modulation treatment techniques for tangential breast irradiation. *Int J Radiat Oncol Biol Phys* 1999;45:1305–14.
5. Lo YC, Yasuda G, Fitzgerald TJ, Urie MM. Intensity modulation for breast treatment using static multi-leaf collimators. *Int J Radiat Oncol Biol Phys* 2000;46:187–94.
6. Donovan EM, Johnson U, Shentall G, Evans PM, Neal AJ, Yarnold JR. Evaluation of compensation in breast radiotherapy: a planning study using multiple static fields. *Int J Radiat Oncol Biol Phys* 2000;46:671–9.
7. de la Torre N, Figueroa CT, Martinez K, Riley S, Chapman J. A comparative study of surface dose and dose distribution for intact breast following irradiation with field-in-field technique vs. the use of conventional wedges. *Med Dosim* 2004;29:109–14.
8. Fan Y, Nath R. Intensity modulation under geometrical uncertainty: a deconvolution approach to robust fluence. *Phys Med Biol* 2010;55:4029–45.
9. Schwarz M, Van der Geer J, Van Herk M, Lebesque JV, Mijnheer BJ, Damen EM. Impact of geometrical uncertainties on 3D CRT and IMRT dose distributions for lung cancer treatment. *Int J Radiat Oncol Biol Phys* 2006;65:1260–9.
10. Bos LJ, van der Geer J, van Herk M, Mijnheer BJ, Lebesque JV, Damen EM. The sensitivity of dose distributions for organ motion and set-up uncertainties in prostate IMRT. *Radiother Oncol* 2005;76:18–26.
11. Jain P, Marchant T, Green M, Watkins G, Davies J, McCarthy C, et al. Inter-fraction motion and dosimetric consequences during breast intensity-modulated radiotherapy (IMRT). *Radiother Oncol* 2009;90:93–8.

Esophagus (2011) 8:9–29
DOI 10.1007/s10388-011-0266-8

SPECIAL ARTICLE

Comprehensive Registry of Esophageal Cancer in Japan, 2003

Soji Ozawa · Yuji Tachimori · Hideo Baba · Mitsuhiro Fujishiro · Hisahiro Matsubara · Hodaka Numasaki · Tsuneo Oyama · Masayuki Shinoda · Hiroya Takeuchi · Otsuo Tanaka · Teruki Teshima · Harushi Udagawa · Takashi Uno · J. Patrick Barron

Published online: 24 February 2011

Preface

We are very pleased to publish the Comprehensive Registry of Esophageal Cancer in Japan, 2003, and thank all the members of the Japan Esophageal Society who made great contributions in preparing this material.

We would like to review the history of the registry of esophageal cancer cases in Japan. The Registration Committee for Esophageal Cancer, the Japan Esophageal Society, has annually registered cases of esophageal cancer since 1976 and published the first issue of the Comprehensive Registry of Esophageal Cancer in Japan in 1979. The Act for the Protection of Personal Information was promulgated in 2003, and began to be enforced in 2005. The purpose of this Act is to protect the rights and interests of individuals while taking into consideration the usefulness of personal information, keeping in mind the remarkable increase in the use of personal information arising from the development of today's advanced information and communications society. The registry of esophageal cancer cases has required some adjustments to comply with the Acts. The new registration system has been discussed for several years and was finally completed in 2008. The most important point was

These data were first issued on 1 March, 2011, as the Comprehensive Registry of Esophageal Cancer in Japan, 2003. Not all pages are reprinted here; however, the original table and figure numbers have been kept.
The authors were at the time members of the Registration Committee for Esophageal Cancer, the Japan Esophageal Society, and made great contributions in preparing this material.

S. Ozawa (✉)
Department of Gastroenterological Surgery,
Tokai University School of Medicine,
143 Shimokasuya, Isehara, Kanagawa 259-1193, Japan
e-mail: sozawa@tokai.ac.jp

Y. Tachimori
Department of Surgery,
National Cancer Center Hospital, Tokyo, Japan

H. Baba
Department of Gastroenterological Surgery,
Graduate School of Medical Sciences Kumamoto University,
Kumamoto, Japan

M. Fujishiro
Department of Endoscopy and Endoscopic Surgery,
Graduate School of Medicine,
University of Tokyo, Tokyo, Japan

H. Matsubara
Department of Frontier Surgery, Graduate School of Medicine,
Chiba University, Chiba, Japan

H. Numasaki · T. Teshima
Department of Medical Physics and Engineering,
Osaka University Graduate School of Medicine, Osaka, Japan

T. Oyama
Department of Gastroenterology,
Saku General Hospital, Nagano, Japan

M. Shinoda
Department of Thoracic Surgery,
Aichi Cancer Center Hospital, Aichi, Japan

H. Takeuchi
Department of Surgery,
Keio University School of Medicine, Tokyo, Japan

O. Tanaka
Department of Surgery, Niigata Cancer Center Hospital,
Niigata, Japan

"anonymity in an unlinkable fashion" using encryption with a hash function. Finally, the registry resumed registering cases of esophageal cancer that had been treated in 2001.

In the Comprehensive Registry in 2003, we newly inserted Figure 3: Survival of patients treated by EMR/ESD in relation to the pathological depth of tumor invasion (pT); Figure 4: Survival of patients treated by EMR/ESD in relation to the lymphatic or blood vessel invasion, in order to present the treatment outcome depending on the pathological status.

We briefly summarized the Comprehensive Registry of Esophageal Cancer in Japan, 2003. A total of 4659 cases were registered from 199 institutions in Japan. Comparing the Comprehensive Registry in 2003 to the Comprehensive Registry in 2002, the number of registered cases and surgical cases increased by 378 and 509, respectively, although the number of registered institutions decreased by 23. As for the histologic type of cancer according to biopsy specimens, squamous cell carcinoma and adenocarcinoma accounted for 92.2% and 3.0%, respectively. Regarding clinical results, the 5-year survival rates of patients treated using endoscopic mucosal resection, concurrent chemoradiotherapy, radiotherapy alone, chemotherapy alone, or esophagectomy were 80.0%, 21.9%, 30.3%, 3.0%, and 46.6%, respectively. Concerning the approach used to perform an esophagectomy, 15.5% of the cases were performed endoscopically, that is, thoracoscopically, laparoscopically, or mediastinoscopically. Regarding the reconstruction route, the posterior mediastinal, the retrosternal, and the intrathoracic route were used in 37.3%, 33.3% and 15.7% of cases, respectively. The operative mortality was 1.0% (25 out of 2510 cases).

We hope that this Comprehensive Registry of Esophageal Cancer in Japan for 2003 helps to improve all aspects of the diagnosis and treatment of esophageal cancer.

Contents

H. Udagawa
Department of Gastroenterological Surgery,
Toranomon Hospital, Tokyo, Japan

T. Uno
Department of Radiology, Graduate School of Medicine,
Chiba University, Chiba, Japan

J. Patrick Barron
International Communications Center,
Tokyo Medical University, Tokyo, Japan

I. Clinical factors of esophageal cancer patients treated in 2003

Institution-registered cases in 2003

Institution
Aichi Cancer Center
Aizawa Hospital
Akita University Hospital
Asahikawa Kosei general Hospital
Asahikawa Medical College Hospital
Chiba Cancer Center
Chiba Prefecture Sawara Hospital
Chiba University Hospital
Dokkyo Medical University Hospital
Foundation for Detection of Early Gastric Carcinoma
Fuchu Hospital
Fujioka General Hospital
Fujita Health University
Fujita Health University Banbuntane Hotokukai Hospital
Gunma Central General Hospital
Gunma University Hospital
Hachinohe City Hospital
Hachioji Digestive Disease Hospital
Hakodate Goryokaku Hospital
Hamamatsu University School of Medicine, University Hospital
Health Insurance Naruto Hospital
Hiratsuka City Hospital
Hiratsuka Kyosai Hospital
Hiroshima City Asa Hospital
Hiroshima University Research Institute for Radiation Biology Medicine
Hofu Institute of Gastroenterology
Hokkaido University Hospital
Hyogo Cancer Center
Hyogo College Of Medicine
Ida Municipal Hospital
Inazawa City Hospital
International University of Health and Welfare Mita Hospital
Ishikawa Kenritsu Chuo Hospital
Ishinomaki Red Cross Hospital
Iwakuni Clinical Center
Iwakuni Medical Center
Iwate Medical University Hospital
JFE Kenpo Kawatetsu Chiba Hospital
Jichi Medical University Hospital
Juntendo University Hospital
Juntendo University Shizuoka Hospital
Kagawa Prefectual Central Hospital
Kagawa University Hospital
Kagoshima Kenritsu Satsunan Hospital
Kagoshima University Hospital
Kanagawa Cancer Center
Kanazawa University Hospital
Kansai Rosai Hospital
Kashima Rosai Hospital
Kashiwa Kousei General Hospital
Kawasaki Medical School Hospital
Keio University Hospital

continued

Institution
Keiyukai Sapporo Hospital
Kikuna Memorial Hospital
Kin-ikyo Chuo Hospital
Kinki Central Hospital
Kinki University Hospital
Kinki University Nara Hospital
Kinki University Sakai Hospital
Kiryu Kosei General Hospital
Kitakyushu Municipal Medical Center
Kitano Hospital
Kitasato University Hospital
Kitasato University Kitasato Institute Medical Center Hospital
Kobe City Medical Center General Hospital
Kobe University Hospital
Kumamoto University Hospital
Kurashiki Central Hospital
Kurume University Hospital
Kuwana City Hospital
Kyorin University Hospital
Kyoto University Hospital
Kyushu University Hospital
Matsuda Hospital
Matsudo City Hospital
Matsushita Memorial Hospital
Matsuyama Red Cross Hospital
Mie University Hospital
Minoh City Hospital
Mito Red Cross Hoapital
Murakami General Hospital
Nagano Red Cross Hospital
Nagaoka Chuo General Hospital
Nagayoshi General Hospital
Nagoya City University Hospital
Nagoya Daiichi Red Cross Hospital
Nagoya University Hospital
Nanpuh Hospital
Nara Medical University Hospital
National Cancer Center Hospital
National Cancer Center Hospital East
National Defense Medical College Hospital
National Hospital Organization Chiba Medical Center
National Hospital Organization Kure Medical Center
National Hospital Organization Kyushu Cancer Center
National Hospital Organization Matsumoto National Hospital
National Hospital Organization Nagano Medical Center
National Hospital Organization Nagasaki Medical Denter
National Hospital Organization Osaka National Hospital
National Hospital Organization Tokyo Medical Center

continued

Institution
Nihon University Itabashi Hospital
Nihonkai General Hospital
Niigata City General Hospital
Niigata Prefectural Shibata Hospital
Niigata University Medical and Dental Hospital
Nikko Memorial Hospital
Nippon Medical School Hospital
Nippon Medical School Musashi Kosugi Hospital
Nippon Medical School Tama Nagayama Hospital
Nishi-Kobe Medical Center
NTT East Japan Kanto Hospital
NTT West Osaka Hospital
Numazu City Hospital
Ohta General Hospital Foundation Ohta Nishinouchi Hospital
Oita Red Cross Hospital
Okayama Saiseikai General Hospital
Okayama University Hospital
Onomichi Municipal Hospital
Osaka City University Hospital
Osaka Koseinenkin Hospital
Osaka Medical Center for Cancer and Cardiovascular Diseases
Osaka Medical College Hospital
Osaka Prefectural Hospital Organization Osaka General Medical Center
Osaka University Hospital
Otsu Red Cross Hospital
Red Cross Society Onoda Hospital
Saga University Hospital
Saiseikai Narashino Hospital
Saitama City Hospital
Saitama Medical Center Jichi Medical University
Saitama Medical University Hospital
Saitama Medical University International Medical Center
Saitama Red Cross Hospital
Saitama Social Insurance Hospital
Saku Central Hospital
Sano Kousei General Hospital
Seirojika National Hospital University Hospital
Sendai City Hospital
Sendai Medical Center
Shiga Medical Center for Adults
Shiga University of Medical Science Hospital
Shikoku Cancer Center
Shimane University Hospital
Shimizu Welfare Hospital
Shinshu University Hospital
Shizuoka City Shimizu Hospital
Shizuoka City Shizuoka Hospital